PERGAMON

International Journal of Multiphase Flow 28 (2002) 1719–1736

International Journal of Multiphase Flow

www.elsevier.com/locate/ijmulflow

Experimental study of two-phase flow in three sandstones. I. Measuring relative permeabilities during two-phase steady-state experiments

Esam Dana [a,b], Frédéric Skoczylas [a,c,*]

[a] *Laboratoire de Mécanique de Lille (URA CNRS 1441), 59650 Villeneuve d'Ascq, France*
[b] *Department of Civil Engineering, Ecole Universitaire d'ingénieurs de Lille, 59650 Villeneuve d'Ascq, France*
[c] *Ecole Centrale de Lille, B.P. (48), 59651 Villeneuve d'Ascq cedex 1, France*

Received 29 March 2001; received in revised form 12 August 2002

Abstract

Hysteretic relative permeability curves for three different sandstones were determined during two-phase steady-state experiments. On the one hand, the experimental device designed and developed is inspired, according to the manner in which the end effects are reduced, by the Penn–State method. On the other hand, semi-permeable membranes were used upstream of the flow to separate the two fluids (gas and liquid) injected. Having corrected the gas relative permeability curves for the Klinkenberg effect, our present results were compared to that obtained previously using a modified version of the transient pulse-decay method with two different saturating liquids. Gas relative permeability curves obtained by this method or by steady-state experiments, where both fluids are mobile, have shown good agreement. Thus, one can conclude that gas effective permeability does not depend, neither, on the percolating liquid or on its mobility and that viscous coupling effects are negligible for such type of flows.

Saturation history has proved to have more influence on the gas relative permeability than on that of the wetting phase. We finally show that result analysis, along with pore structure information accessible from mercury intrusion tests, would enable the specification of a pore entry radii range, controlling the steep part of the relative permeability curves. For sandstone samples tested here, these pores are of comparable sizes.

Keywords: Experiments; Relative permeability; Hysteresis; Steady-state regime; Transient regime; Mercury porosimetry; Pore structure

* Corresponding author. Address: Ecole Centrale de Lille, B.P. (48), 59651 Villeneuve d'Ascq cedex 1, France. Tel.: +33-3-20-33-53-64; fax: +33-3-20-33-53-52.

E-mail addresses: esam.dana@eudil.fr (E. Dana), frederic.skoczylas@ec-lille.fr (F. Skoczylas).

0301-9322/02/$ - see front matter
PII: S0301-9322(02)00090-3

1. Introduction

Concomitant flow of various fluid phases in porous media is observed in a considerable number of engineering applications such as: petroleum engineering, sciences and technology of environment, etc. Simultaneous flow of different fluid phases can be classified according to the flow mode (i.e., transient or steady-state), to the type of fluids (i.e., miscible or not), or to whether these fluids run out in the same direction (co-current flow) or in opposite directions (counter-current flow) (Dullien, 1992; Kaviany, 1991; Bear, 1988).

Some particular difficulties are encountered while observing equilibrium states in porous media as they are characterized by the fluid distribution in the pore space which depends on many parameters such as: geometry and topology of porous space (connectivity, interface geometry), the chemical composition of the rocks and fluids (via the surface tension and the contact angle, for example), the movement which preceded balance (history of saturation) (Dullien, 1992; Kaviany, 1991; Marle, 1981; Houpeurt, 1974). Given these difficulties, a macroscopic approach, based on a generalized form of Darcy's law, is commonly used. According to this approach, biphasic flow is completely described by relative permeability coefficients and capillary pressure relating the pressures in both phases (Dullien, 1992; Marle, 1981). Considering that the various forces acting on both sides of the fluid–fluid interface (fluid–fluid coupling) can play an important role in this type of flow, a coupled form of Darcy's law has been proposed by several authors and following different theoretical backgrounds (Kalaydjian, 1990; Whitaker, 1986; Auriault and et Sanchez-Palencia, 1986). These reveal, in addition to the two relative permeability coefficients, two viscous coupling coefficients which depend, as relative permeabilities do, on the characteristics of the system considered: solid matrix/fluide1/fluide2 (Avraam and Payatakes, 1995b; Rose, 1988). However, a suitable method allowing their separation seems to be very difficult. In most of experimental methodologies suggested, the determination of these coefficients is primarily based on relative permeability experiments in the sense of the uncoupled form of Darcy's law (Avraam and Payatakes, 1995b; Kalaydjian, 1990; Rose, 1988). Measurement techniques of relative permeabilities are highly distinctive where validity and reliability of the obtained results are often questioned (Rose, 1987). On the one hand, experimental difficulties, varying from one method to another, are omnipresent, and on the other hand, numerous parameters can influence desired measurements (Richardson et al., 1952; Osoba et al., 1951).

This work mainly concerns the experimental characterization of two-phase flow (liquid and gas phases) in three different sandstones: two Vosges sandstones and a Fontainebleau one. Based on a macroscopic approach, this study is focused on their relative permeability and capillary pressure curves. The influence of certain parameters on the flow type in question such as: the pore size distribution, viscosity of the wetting fluid, history of saturation, and mobility of the wetting phase, occupies a central part of this work.

The first part of this work is devoted to relative permeability measurements. Hereafter, we present the successive parts of this article. First, comes a brief discussion of problems related to this type of experimentation. After explaining the steady-state method used and the designed experimental set-up, experiments conducted on three different sandstones will be presented. Results obtained are then compared with that obtained by Dana and Skoczylas (1999) applying a transient method, for the same three rocks. This point is of particular interest since experimental results comparing steady-state and transient methods are very rare in written sources. Finally,

results will be commented upon and analyzed in parallel with pore space information available from mercury porosimetry curves.

2. Relative permeability measurement

2.1. Measurement technique problems, review of the literature

In a typical steady-state experiment, two fluids are simultaneously injected at constant and known flow rates. Steady-state is supposed as soon as the flow rate upstream is equal to that downstream of the sample and/or if a constant difference in pressure is observed through the sample tested. The establishment of the steady-state can require from 2 to 40 h according to the sample permeability and the method used (Dullien, 1992; Bear, 1988).

It is generally accepted that in steady-state flow experiments conducted over a homogeneous porous medium, uniform saturation can extend over the whole specimen, vicinity of the effluent aside. During laboratory experiments, the percolating fluids pass from a zone in the porous medium where the capillary pressure has a finite value towards an open container where the capillary pressure vanishes. The rock sample tends, by effect of capillary forces, to retain the wetting fluid and thus creates a higher saturation near the downstream of the flow rather than in the remainder of the tested specimen. This phenomenon is called the "capillary end effect" (Richardson et al., 1952). The attenuation of the end effects will allow the assumption of uniform saturation and thereafter: (1) the relative permeability, at a given saturation, is constant all along the sample, following the two-phase form of Darcy's law, and (2) the capillary pressure is uniform also, this implies the same pressure gradients for both fluids. Thus the second major experimental difficulty is to determine the pressure gradients of the two fluids. By allowing their equality, the problem is reduced to measure the difference in pressure in a given phase (often in the non-wetting phase).

Many approaches were used or proposed in order to reduce the capillary end effects, these methods are (Osoba et al., 1951): (1) to take all measurements on a section sufficiently far away from the end of the sample, (2) the use of sufficiently high flow rates (or gradients of pressure), (3) by maintaining the wetting fluid immobile or, (4) by controlling and imposing the same capillary pressure upstream and downstream of the sample.

We may cite as an example, interalia, works of Abbas et al. (1999) and of Ramakrishnan and Capiello (1991) where the method of stationary liquid was employed for determining the non-wetting phase permeability. Avraam and Payatakes (1995a) and Fleureau and Taibi (1994) used two types of semi-permeable membranes, one to the wetting phase and the second to the non-wetting phase, to separately measure the difference in pressure in the injected two fluids. Despite the use of semi-permeable membranes, it proves to be impossible to impose the same difference in pressure in the two fluids (Avraam and Payatakes, 1995b).

2.2. Steady-state measurement: experimental set-up

We present here the experimental set-up designed to measure the relative permeabilities during a steady-state two-phase flow experiment.

On the one hand, the designed experimental device is inspired, according to the manner in which the end effects are reduced by the Penn–State method. On the other hand, semi-permeable membranes were used upstream of the flow to separate the two injected fluids; without these membranes particular difficulties appeared during the experimentation, as we will see in the following. A schematic representation of the test bench is given in Fig. 1.

This assembly includes a non-wetting phase injection circuit (gas), a wetting fluid injection circuit (ethanol), and a testing cell. The gas injection circuit is composed of Argon feed reservoir and of a low-pressure valve allowing the injection and the regulation of the gas pressure. At the sample outlet, the gas flow rate is measured using a set of float flowmeters covering a broad range of flow rates. In the liquid injection circuit, an air reservoir and a control valve are connected to the injection cell so as to regulate and generate the pressure of the wetting phase. The injection flow rate is measured upstream of the sample using a group of high-pressure flowmeters. In our tests, steady-state will thus be deduced from the stabilization of the gas pressures upstream and downstream of the sample and of the observed flow rates of both fluids at the effluent, this constitutes an indication of the absence of end effects (Rose, 1987).

The testing cell is well adapted for the use of cylindrical samples 37 mm in diameter and a wide range of lengths. The central part of the sample, on which measurements are taken (to minimize end effects) and which thereafter will be called sample, is fixed in a metal tube using a synthetic resin allowing easy dismantling and reliable sealing. The inlet face of the sample is in contact with a mixing part (mixer), of the same material as the sample, via which the two fluids are injected, mixed, and uniformly distributed on the injection face of the sample. In order to confine the end effects far away from the sample, its outlet face is connected to a section also made up with the same material (reducer). To improve contact between these three parts, a spring is placed between the cell and the reducer section. The wetting phase is injected through a semi-permeable membrane (hydrophilic), while gas is directly injected into the mixer. At the effluent, both fluids are separated by gravity forces. Maintaining a stationary level of the wetting liquid (Fig. 1) allowed us to ensure that the gas was diffused in the circuit intended for its flow rate measurement (towards the flowmeter) and not in the water recovery piping.

During the experimentation phase, the separation of the injected fluids by the use of semi-permeable membranes (having a breakthrough pressure of 300 kPa) proved to be essential; in the absence of those, the non-wetting fluid, at a higher pressure than that of the wetting phase, was able to penetrate the wetting-liquid injection circuit. Therefore the continuity of the wetting phase is no longer ensured, and flow then became (of pulsatory nature) intermittent. After periods of up to 10 h, steady-state was never established. However the use of these membranes excluded a direct measurement of the pressure in the wetting phase.

The premises in which the testing bench is located were maintained at a constant temperature of 20 °C to avoid the influence of temperature fluctuations.

2.3. General testing principles and procedure

The three parts of the sample are saturated with ethanol (i.e. the wetting-phase) and placed in the testing cell as illustrated in Fig. 1. We begin the experiment by liquid injection, the flow rate and the difference in pressure are measured to determine the intrinsic permeability of the tested rock. The second stage consists in injecting gas and gradually adjusting its pressure in small steps

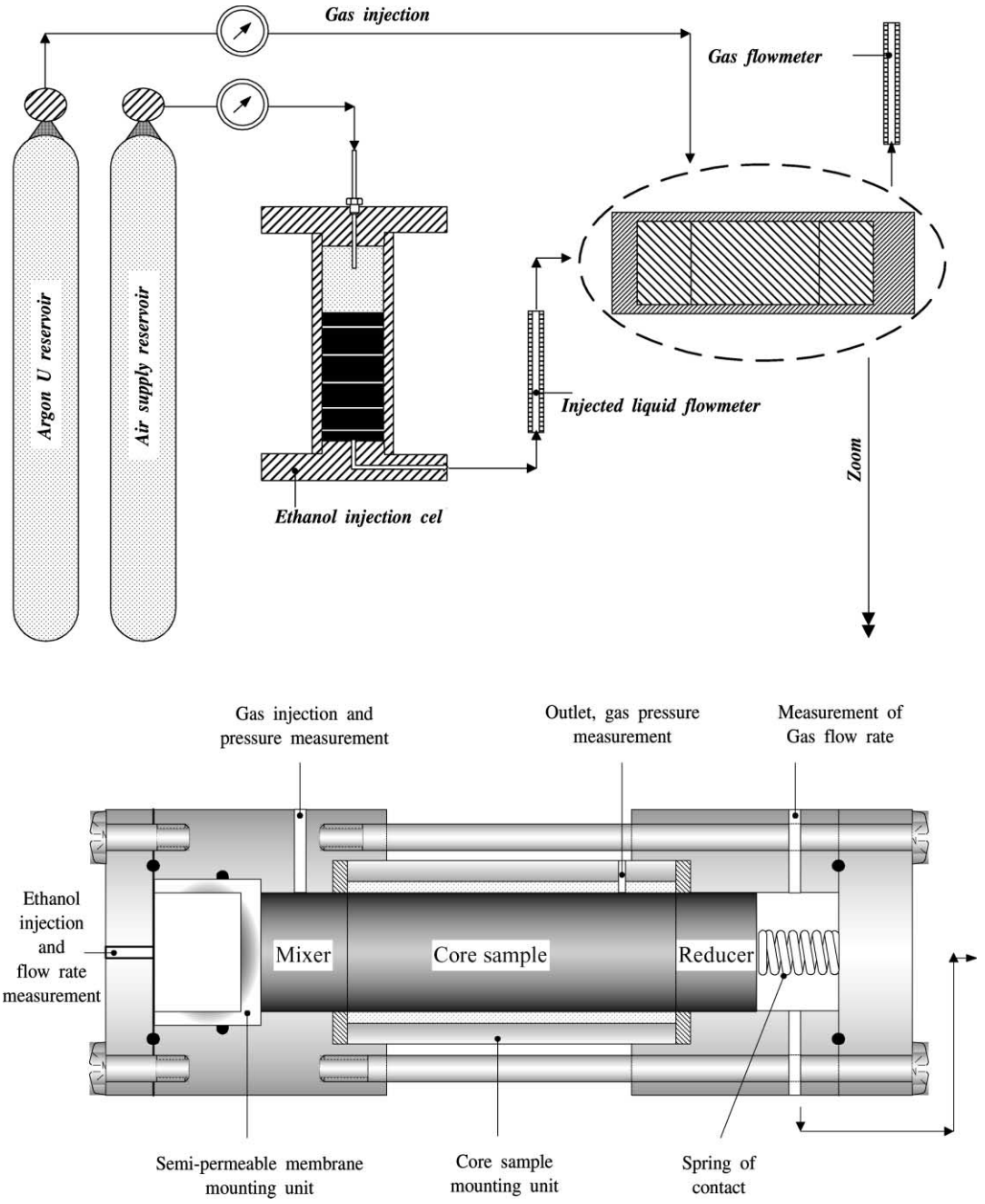

Fig. 1. Schematic representation of the testing bench.

in order to desaturate the sample. To eliminate the possible influences of the pressure gradient, the pressures in the two phases are set so as to obtain a gradient of pressure equal to that of the initial phase of the test. This task is particularly difficult: we accepted in our tests gradients presenting a

difference of 10%. Thereafter, it is necessary to wait from 1 to 2 h to observe the steady-state (stationary pressures and flows). When balance is established the flow rates of the two phases as well as the pressures upstream and downstream of the sample are recorded. The sample is quickly extracted from the cell to be weighed. We determine, in this manner, the degree of saturation corresponding to this state of balance. Fig. 2 shows the positions and the lengths on which measurements are really taken.

The sample is remounted and the testing cell is reassembled. Since the curves of relative permeabilities are often regarded as a succession of equilibrium states, the two phases must be re-injected in the same conditions as in the preceding stage prior to further desaturation of the sample. This is usually done so as to obtain the same geometrical distribution of the two phases in the pore space, which is an 'a priori' assumption (Rose, 1991). The injection ratio Q_{nw}/Q_w is then increased again by slightly adjusting the injection pressures, and the previously described stages are repeated to determine the relative permeabilities corresponding to the new state of balance. The process described above is repeated several consecutive times to determine the whole drainage curves of relative permeability (the wetting phase being displaced by the non-wetting one). From the minimum saturation obtained, we proceed in opposite manner, i.e. by reducing the injection ratio Q_{nw}/Q_w, to determine the imbibition relative permeability curves.

We suppose within the framework of this study that the flow of the fluid obeys the generalized Darcy's law (theory of relative permeability) which for an isotropic medium, is written:

$$Q_i = -\frac{kk_{ri}(S_w)A}{\mu_i}\left(\frac{dP}{dx}\right)_i; \quad i = (w, nw) \tag{1}$$

where Q_i, is the flow rate of phase i (m^3/s), A is the sample cross-section area (m^2), μ_i, is the viscosity of the i phase (Pa s), and $(dP/dx)_i$ is the pressure gradient in phase i (Pa/m). The intrinsic permeability is k (m^2), and the relative permeability to phase i is $k_{ri}(S_w)$ function of the wetting phase saturation S_w. Indices w and nw refer to wetting and non-wetting phases respectively.

We suppose that, when a steady-state regime is established, saturation is uniform, since the end effects are confined away from the central part of the sample where measurements are taken. It follows that a uniform capillary pressure extends along the sample, from which:

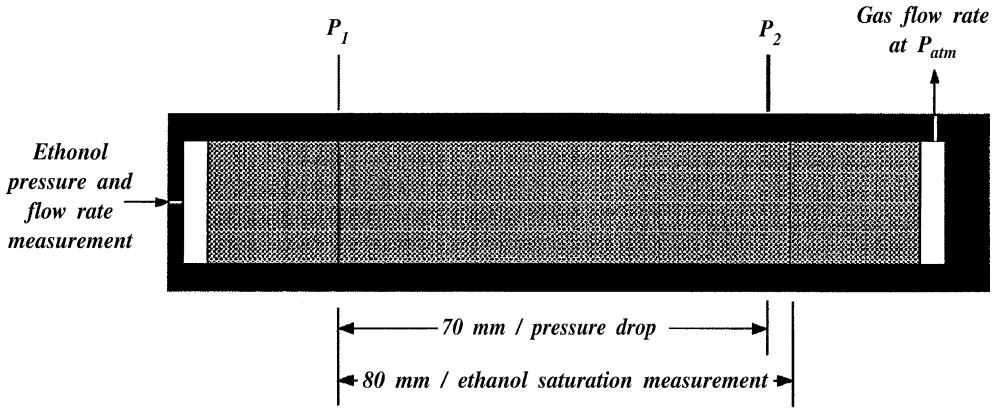

Fig. 2. Real measurements and positions.

$$P_c(\text{inlet}) = P_c(\text{outlet}) \Longleftrightarrow \Delta P_w = \Delta P_{nw} \tag{2}$$

For the case of a unidirectional gas flow through porous media, one can easily show that the pressure profile may be written as (Dana and Skoczylas, 1999):

$$P(x) = \sqrt{P_1^2\left(1 - \frac{x}{L}\right) + P_2^2\left(\frac{x}{L}\right)} \tag{3}$$

Combining Eq. (3) and Darcy's law yields:

$$Q_{g,2} = \frac{kk_{rg}(S_w)A}{\mu_g}(P_{ave}/P_2)(\Delta P/L) \tag{4}$$

with the average pressure $P_{ave} = (P_1 + P_2)/2$, and $Q_{g,2} = (P_{atm}/P_2) \times Q_{measured}$, since the gas flow rate (supposed perfect) is measured, in our assembly, at atmospheric pressure (see Fig. 2).

For the wetting liquid we may write:

$$Q_w = \frac{kk_{rw}(S_w)A}{\mu_w}\frac{(P_1 - P_2)_w}{L}; \quad (P_1 - P_2)_w = (P_1 - P_2)_{nw} \tag{5}$$

This last equation constitutes the main assumption justified by the absence of capillary end effects.

2.4. Materials and experimental results

Table 1 summarizes the principal characteristics of the tested rock. The tests were carried out with cylindrical samples 37 mm in diameter and 80 mm length. The difference in pressure is measured over the central part of the core sample (70 mm length), whereas saturation is given over the whole length (Fig. 2). The mixer and reducer sections are 20 mm length. Measurements of pressure are thus performed on 70% of the total length of the central part and the reducer section. Argon U of above 99% purity as the injection gas and ethanol of 99.7% purity as the liquid of saturation were employed (Table 2) to perform the tests. Ethanol, which is the wetting phase, was used instead of water to avoid clogging the used membranes with bacteria development. The initial pressure of alcohol injection is fixed for all the tests at 200 relative kPa yielding a difference in pressure of about 80–100 kPa according to the permeability of the sample tested. During the developed biphasic flows this difference in pressure is maintained at its initial value by adjusting the two injection pressures, variations of about 10%, however, were tolerated.

Macroscopic capillary number, i.e. ratio of viscous to capillary forces, rising from testing conditions can be calculated as $N_{ca} = (\mu V/\sigma) \approx (\text{kGradP}/\sigma)$ where σ is the interfacial tension.

Table 1
Tested rock characteristics

	ρ_B	ρ_S	ϕ_{total}	S_{BET}	k
Vosges-1	2.15	2.59	17	0.64	5.0×10^{-13}
Vosges-2	2.06	2.57	20	3.10	2.0×10^{-14}
Fontaine	2.36	2.60	9.5	0.03	2.0×10^{-13}

ρ_B, ρ_S are, respectively, the bulk and skeletal density (g/cm^3), ϕ_{total} is the total porosity (%), S_{BET} is the specific surface (m^2/g), and k is the average intrinsic permeability (m^2) of the core sample.

Table 2
Utilized fluid characteristics at 20 °C

	Viscosity (cP)	Surface tension (mN/m)	Viscosity ratio μ_g/μ_l
Argon	0.0226	–	–
Water	1.0	72.8	0.0226
Ethanol	1.2	22.3	0.0188
Glycol ethylene	21.4	47.7	0.00106

Table 3
Capillary numbers

Fontainebleau	Vosges-1	Vosges-2
$N_{ca} = 1.2 \times 10^{-5}$	$N_{ca} = 3.0 \times 10^{-5}$	$N_{ca} = 1.2 \times 10^{-6}$

The numbers obtained (see Table 3) for the tested rocks can be seen as limit values for rock-reservoir type where relative permeability and capillary pressure are independent of flow rate (Osoba et al., 1951; Richardson et al., 1952).

2.4.1. Relative permeability hysteresis

Imbibition relative permeability curves are directly determined after drainage, starting from the last degree of saturation approached in the cycle which precedes it. Fig. 3(a)–(f) illustrates the dependence of the relative permeabilities on the history of saturation.

2.4.2. Steady-state versus transient method

Now we will compare the gas relative permeability curves obtained by the steady-state technique presented above to that obtained by Dana and Skoczylas (1999) using a pulse-test technique, shortly presented here. The general principles of testing conditions are to subject the cylindrical sample, whose saturation is checked by drying and accurate weighing, to a low confining pressure and static gas pressure on its upper and lower surfaces (the saturating fluid is thus held stationary), followed by the application of a slight excess of pressure to one of the sides, and to record over a period of time the evolution in the difference of pressure between the two surfaces. Based on these recorded data, the method used allows the relative permeability to be evaluated via certain simplifications or numerical (and/or analytical) processing. It was supposed that the fluid flow obeys Darcy's law. The flow is sufficiently slow to be considered as laminar and the static pressure sufficiently high (2 MPa) for the Klinkenberg effect to be ignored (Iffly, 1956). The same injection gas as here was used with glycol ethylene (see Table 2) or water as the wetting phase. The authors reported no influence of saturating fluid on gas relative permeability. Further details may be found in Dana (1999) or Dana and Skoczylas (1999). An example of these results is given on Fig. 4.

Given the difference observed in the Fontainebleau sandstone samples, overhead are only compared gas relative permeability curves obtained for the Vosges-1 and Vosges-2 sandstones by the two methods employed (pulse-test/steady-state flow). Nevertheless, the above results provide

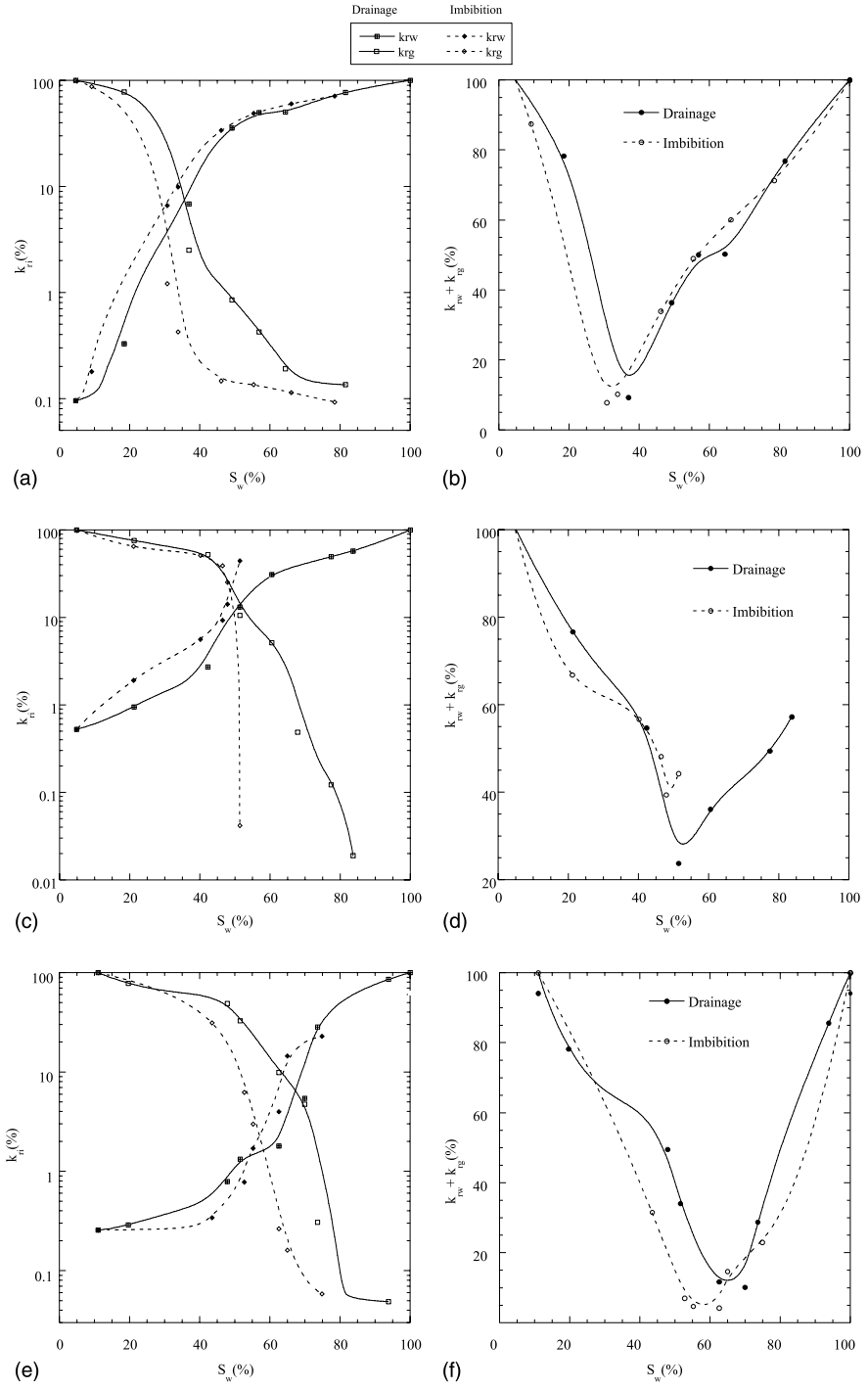

Fig. 3. Relative permeability hysteresis curves for the tested rocks: (a) Fontainebleau sandstone; (b) relative permeability sum; (c) Vosges-1 sandstone; (d) relative permeability sum; (e) Voltage-2 sandstone; (f) relative permeability sum.

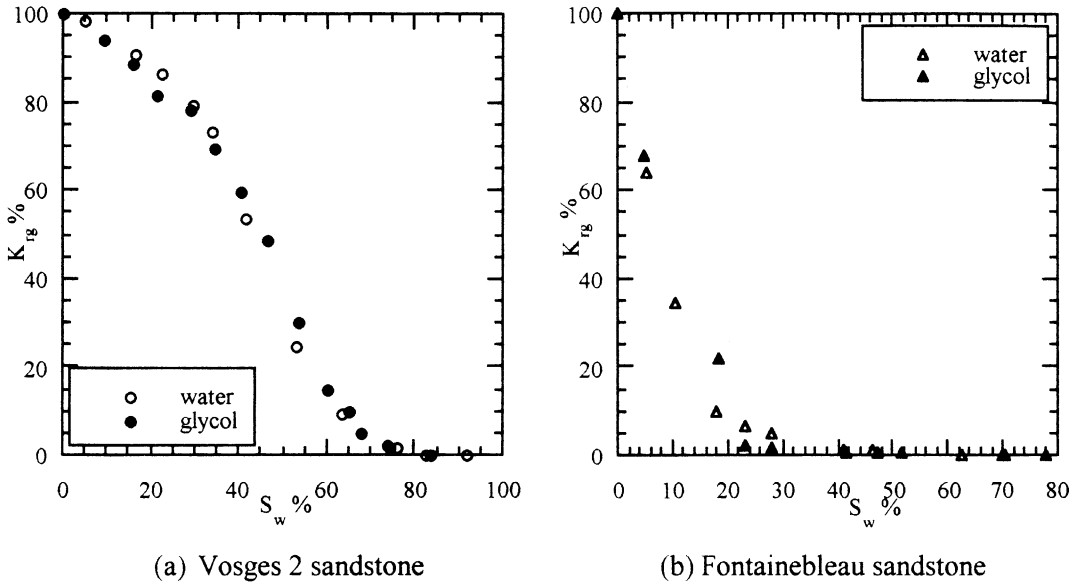

Fig. 4. Gas relative permeability (pulse test). Effect of saturation liquid: (a) Vosges-2 sandstone; (b) Fontainebleau sandstone.

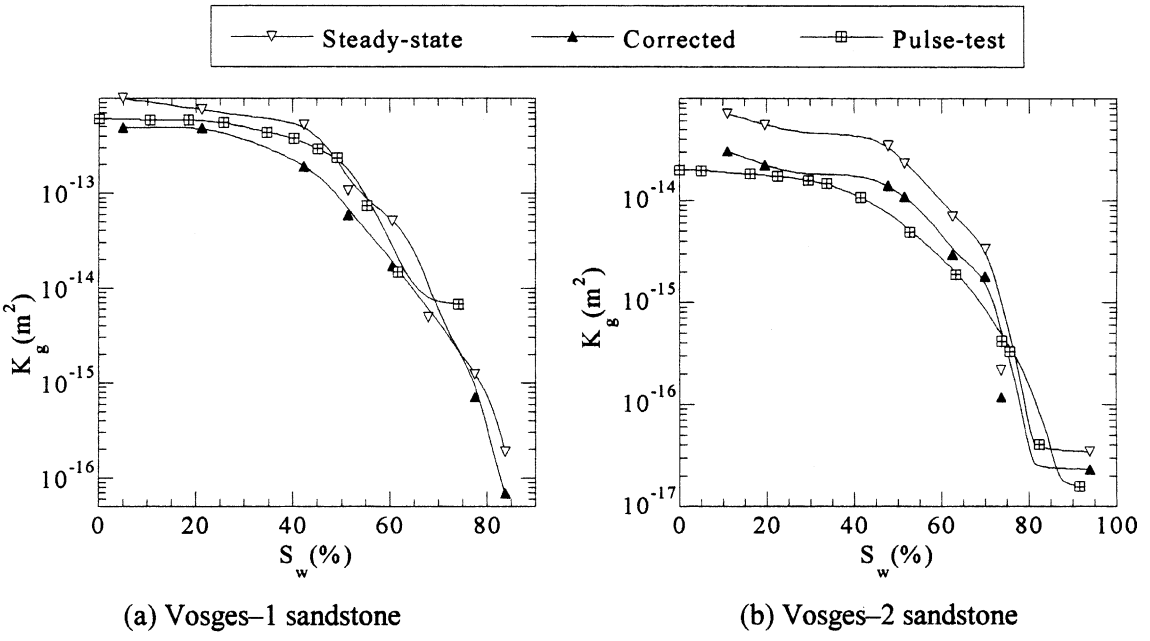

Fig. 5. Steady-state versus pulse-test method and correction for the Klinkenberg effect: (a) Vosges-1 sandstone; (b) Vosges-2 sandstone.

strong evidence of similarity of gas relative permeabilities determined under different flow conditions.

The first comparison showed that the effective permeability to gas determined by the stationary method is higher than that arising from the pulse technique (Fig. 5). Indeed, the experiments in steady-state were carried out at low gas pressure leading to an additional gas flow due to the slip phenomenon (Klinkenberg effect).

The Klinkenberg equation takes into consideration this effect and can be written in the form (Dullien, 1992):

$$k_a = k(1 + b/P_{ave}) \tag{6}$$

where k_a is the apparent gas permeability and b is a constant characteristic of the gas and the porous medium.

To obtain the constant b, several intrinsic gas permeability tests have been performed at various average gas pressures on completely dried samples. Nevertheless a biphasic flow leads to a different situation as the constant b can vary with sample saturation and thus requiring numerous tests (at different degrees of saturation). Given the weak influence of b (about 100 kPa, for our three sandstones) in the zone of low and average gas saturations (Fig. 5), a unique value was used to correct the gas relative permeability in all saturation ranges.

3. Result analysis

We will begin by presenting and analyzing the pore structure information arising from mercury porosimetry curves given in Fig. 6.

The Fontainebleau sandstone has a porosity which is much more homogeneous than that of the other sandstones; the mercury intrusion curves (Fig. 6) indicate the small part the pores of entry radius $R < 1$ (μm) play in its total porosity. The porosity of this sandstone is primarily concentrated in the vicinity of the peak of the curve of intrusion.

Contrary, to the Fontainebleau sandstone, the mercury intrusion curves of the two Vosges sandstones show that the small pores constitute a significant fraction of their total porosity. The specific surface determined by the BET method also states that the presence of small pores in the Vosges-2 sample ($S_S \approx 3.10$ m^2/g) is more significant than in Vosges-1 ($S_S \approx 0.64$ m^2/g). Nevertheless, the pore size distribution of these two sandstones is mainly different in the vicinity of the peak and can be regarded as similar in the field of small pores (Fig. 6(a)). This results in discernible differences in their cumulated porosity curves (Fig. 6(b)).

3.1. Wetting and non-wetting phase relative permeability during drainage

As one can observe on Fig. 3, the ethanol relative permeability (which will refer to the wetting phase from now on) varies slightly with the saturation history which is not the case for the gas permeability with a more pronounced hysteretic effect.

Given that the tested sandstones have different porosities (average and distribution), presenting the relative permeability curves as a function of the mere saturation degree would lead to incorrect interpretations. This is illustrated on Fig. 7 where saturation variation is depicted as a function of pore entry size.

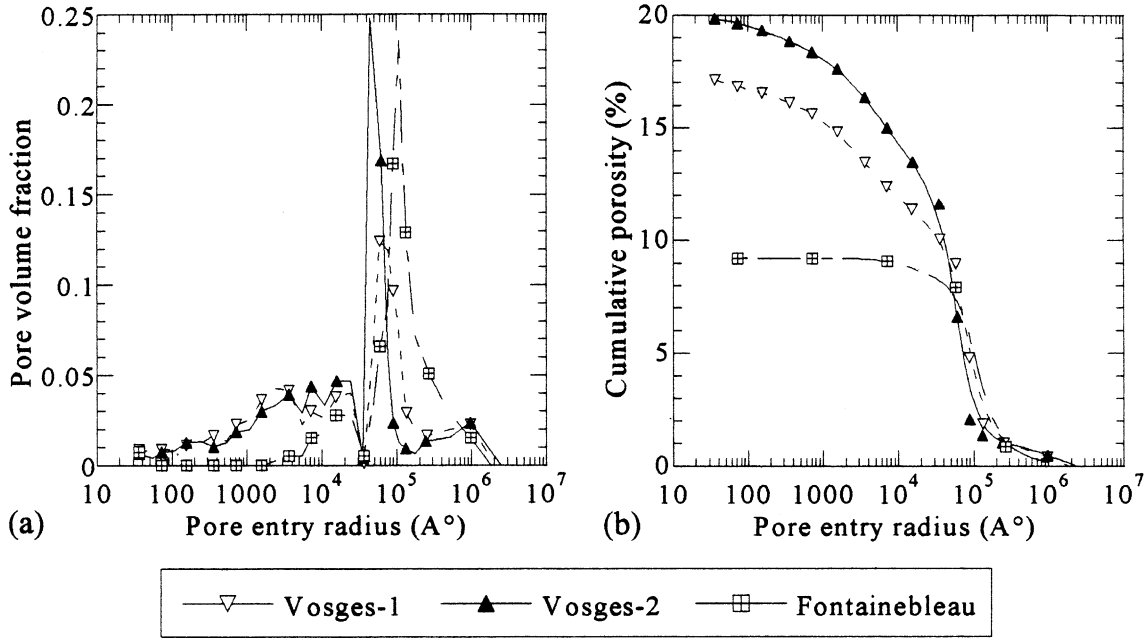

Fig. 6. (a) Pore size distribution. (b) Cumulative porosity curves.

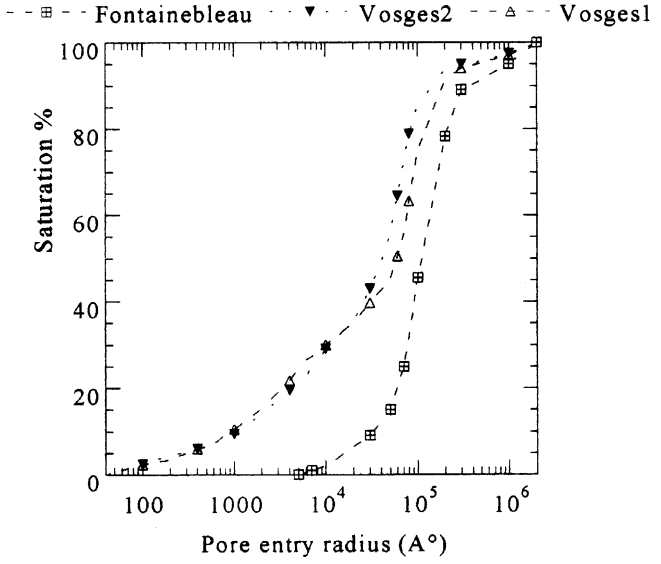

Fig. 7. Saturation versus pore entry radius.

As mentioned earlier, and as clearly readable from figures above, the Fontainebleau sample presents a relatively homogeneous porosity, vanishing for pore radii smaller than 1 μm. Though the apparent resembling curves for the two Vosges sandstones, contrast in saturation corres-

ponding to pore radii still persists. On Fig. 7, one would observe the slightly finer porosity of the Vosges-2 sandstone compared with the other tested sandstones.

Gas and liquid relative permeabilities as a function of pore entry radius are depicted on Figs. 8–10. From its inception, gas injection is noticed to decrease the wetting phase permeability

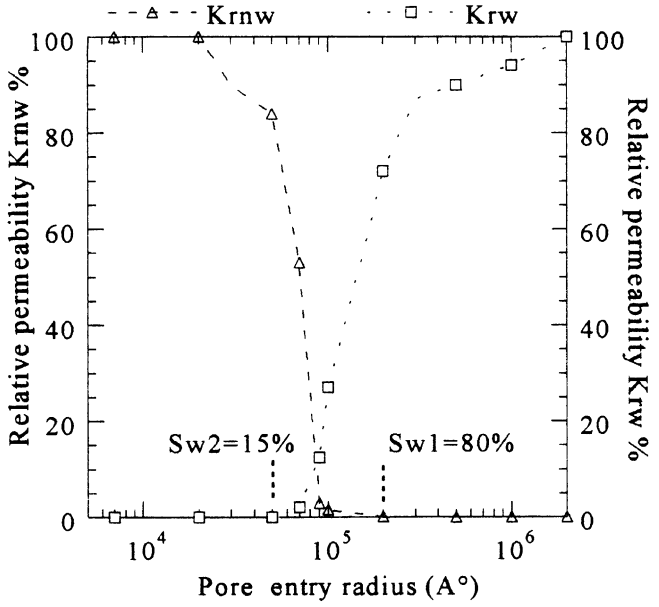

Fig. 8. Relative permeability variations versus pore entry radius Fontainebleau Sandstone.

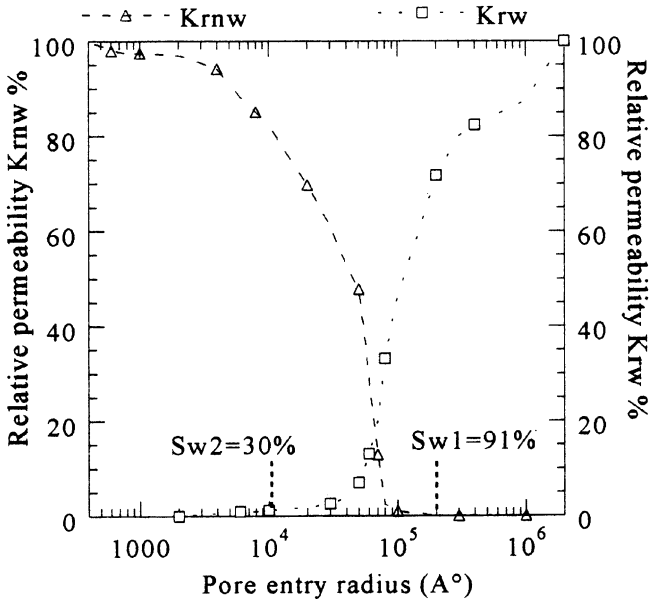

Fig. 9. Relative permeability variations versus pore entry radius Vosges-1 Sandstone.

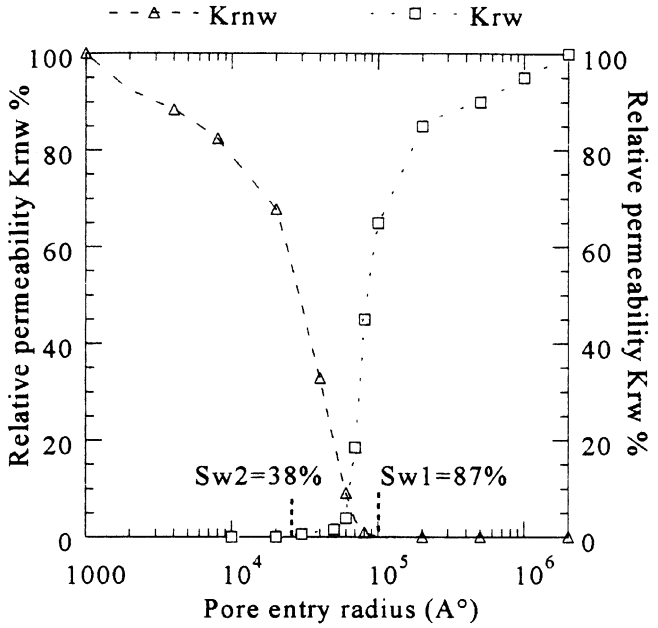

Fig. 10. Relative permeability variations versus pore entry radius Vosges-2 Sandstone.

(K_{rw}) in the absence of gas breakthrough across the sample. This stage is characterized by gas being trapped and resisting to liquid phase percolation. Gas breakthrough will only initiate after drainage of pores having entry radii within the range 10^5–2×10^5 Å. These values, marked as S_{w1} on Figs. 8–10, also point out a decrease of 30% in K_{rw}.

As soon as gas starts to span the sample, a drastic decline of the K_{rw} is observed (Fig. 11). Further drainage will lead pores of size between 10^5 and 10^4 Å to be desaturated and gas relative permeability is as high as 80–100%. Drainage of pores characterized by entry radius less than 10^4 Å reveals no effect in K_{rw}. At these peculiar points, designated as S_{w2} on Figs. 8–10, residual saturation is specified, values of which, for the three sandstones, are given in tabular form (Table 4). It is in the range S_{w1}–S_{w2} that the concept of relative permeability would be completely pertinent, the two fluid phases are, indeed, flowing. For our sandstones, shortcomings of experimental precision and dispersion kept in mind, this range corresponds to pores having size going from 10^5 to 10^4 Å.

The bottom row of Table 4 gives the pore entry radius corresponding to the residual saturation. The relatively low residual saturation of the Fontainebleau sandstone rises from its large and homogeneous porosity compared to the Vosges sandstones (Fig. 7).

3.2. Gas relative permeability

Fig. 5 shows that the Klinkenberg effect plays a significant role only in the field of low and average saturation ($S_w < 50\%$), i.e. the broadest pores present in the three rocks tested have a greater size compared to the mean free path of the gas molecules. The previous analysis of the

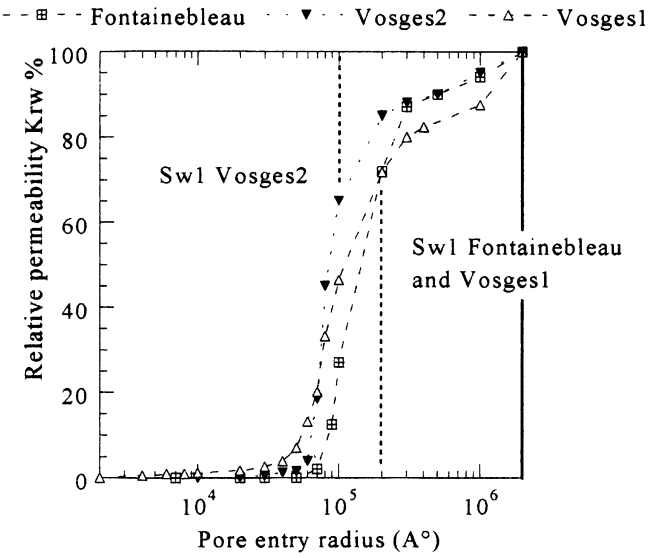

Fig. 11. Relative permeability variations K_{rw} versus pore entry radius.

Table 4
Residual liquid saturation—drainage phase

Grès	Fontainebleau	Vosges-1	Vosges-2
S_{irr} (%)	15	30	38
Entry radius at S_{irr} (Å)	$\approx 5 \times 10^4$	$\approx 10^4$	$\approx 2 \times 10^4$

pore space showed us that the Vosges-2 sandstone presents a fraction of fine porosity that is more significant than that of the two other sandstones; the slip phenomenon appeared to be more important than in the other two rocks (see Fig. 5).

After taking into account the Klinkenberg effect, the experimental results of the gas relative permeability (in drainage) resulting from measurements in steady or transitory state can be regarded as identical and this for the two Vosges sandstones (Fig. 5). A detailed analysis of these curves is given in Dana and Skoczylas (1999).

The curves of effective permeability to gas during drainage, of the two Vosges samples, by the both techniques, are compared in Fig. 5. This comparison shows good agreement in the results obtained.

The tests carried out with water or ethylene glycol by Dana and Skoczylas (1999) show that the gas relative permeability remains unchanged when the viscosity of the saturating fluid is 20 times higher than that of water (Fig. 4). In tests using the pulse-test technique, the saturating fluid is stationary on a macroscopic scale. This was systematically checked by weighing the sample before and after the test. This observation indicates that the permeability to gas, and more generally to the non-wetting phase, is independent of the main properties (viscosity, specific mass, superficial tension) of the wetting fluid when the later is immobile inside the pore space. In addition, Fig. 5 shows that gas effective permeability (accordingly, relative), whether measured using pulse-test

(with water or ethylene glycol) or using the steady-state technique (with ethanol), remains substantially the same. This feature provides strong evidence that fluid–fluid coupling effects are negligible and that the gas relative permeability is pertinently expressed as a function of the only degree of saturation. A second observation—on the scale of pores—stems from the fact that, in our specific case, the wetting phase physical properties do not play a relevant role in determining the gas relative permeability, implying that at a given saturation degree, gas will flow through the same fraction of pore structure leading to similar gas permeability curves (macroscopic parameter). Moreover the obtained correspondence for gas relative permeability measured by the steady-state technique (wetting phase is flowing) or by the pulse-test (wetting-phase held stationary) show clearly that the mobility of the wetting phase would have no influence on gas relative permeability.

3.3. Relative permeabilities and history of saturation

The dependence of the relative permeability on the history of saturation was previously presented in Fig. 3. It appears that the water relative permeability of the Vosges-1 sandstone is influenced more by the history of saturation than those of the other sandstones. In drainage, the sum of the relative permeabilities can reach values as low as 10% for the Vosges-2 samples and Fontainebleau, and 15% for the Vosges-1 sample (Fig. 3(b), (d), and (f)). In drainage or imbibition, the water relative permeability equivalence indicates similar pore space fraction occupied by water during the flow. In imbibition, the gas relative permeability curves are located to the left of those of drainage and present a variation that is faster than the drainage curves (Fig. 3). The pores governing the permeability to gas are thus characterized by sizes that are lower than those of the dominant pores in drainage. These pores can be identified with the pore throats where the disconnection and the trapping of the non-wetting phase by snap-off takes place.

4. Conclusions and perspectives

The present work aimed at direct experimental determination of relative permeability curves. Experimental techniques, principles of which were developed early in the 50s, are usually designed to accommodate materials of high permeability. Measurements are generally conducted under small pressure gradients (i.e. low capillary number) over reasonable time periods. Their major advantage lays in the possibility of gathering, for the sample material, necessary information to describe its behavior under two-phase flow conditions. In the absence of such information, models of "statistical type" are often employed and will be discussed in the second part of the present study.

Relative permeability curves of three sandstones were determined using two distinct techniques: the pulse-test (unsteady) and the dynamic displacement method (steady-state). The later allows measuring the relative permeability to the two circulating fluids, as well as their dependency on history of saturation. Comparisons between these two techniques clearly showed that obtained gas relative permeabilities are very similar. Moreover these experiments have provided strong evidence that gas relative permeability only depends on liquid saturation, the later's physical properties being of negligible effect. Viscous coupling effects, in this case, are clearly of no im-

portance. Analysis of relative permeability curves, along with pore size distribution based on mercury intrusion data, enabled us to underline a ''range of pore sizes'' where the two fluids are actually flowing and where the concept of relative permeability is pertinent. Despite different intrinsic permeabilities, for the sandstones tested here, this range can be considered to be the same (Figs. 8–10). Results also confirm a well known phenomenon that non-wetting phase permeability is much more influenced by hysteresis than that of the wetting phase in a capillary-dominated flow of strongly wetting phases.

The method adopted in this work has the advantage of minimizing uncertainty on the distribution of fluids near the effluent, the way in which the end effects are reduced, and the simplicity of measurements it requires. However, the pressure in the wetting phase is not directly measured, which excludes a simultaneous determination of the capillary pressure curves. The later curves are already measured using the porous plate technique and will be exploited in parallel with three ''Burdine-type'' models; the results will be presented in the second part of this work.

References

Abbas, A., Carcasses, M., Ollivier, J.-P., 1999. Gas permeability of concrete in relation to its degree of saturation. Materials and Structures 32, 3–8.

Auriault, J.-L., et Sanchez-Palencia, E., 1986. Remarque sur la loi de Darcy pour les écoulements biphasiques en milieux poreux. Journal de Mécanique Théorique et appliquée (numéro spécial), 141–156.

Avraam, D.G., Payatakes, A.C., 1995a. Flow regimes and relative permeabilities during steady-state two-phase flow in porous media. Journal of Fluid Mechanics 293, 207–236.

Avraam, D.G., Payatakes, A.C., 1995b. Generalized relative permeability coefficients during steady-state two-phase flow in porous media. Transport in Porous Media 20, 135–168.

Bear, J., 1988. Dynamics of fluids in porous media. Dover Publication Inc., New York.

Dana, E., 1999. Contribution à la caractérisation des écoulements biphasiques dans les matériaux poreux. Etude expérimentale sur trois grès, PhD dissertation, Universitédes Sciences et Technologies de Lille (USTL), Lille, France.

Dana, E., Skoczylas, F., 1999. Gas relative permeability and pore structure of sandstones. International Journal of Rock Mechanics and Mineral Science 36, 613–625.

Dullien, F.A.L., 1992. Porous media: fluid transport and pore structure, second ed. Academic press, San Diego.

Fleureau, J.-M., Taibi, S., 1994. A new apparatus for the measurement of water–air permeabilities, First international congress on environmental geotechnics, July 10–15, Edmonton, Alberta, Canada.

Houpeurt, A., 1974. Mécanique des fluides dans les milieux poreux: critique et recherche, éd. Technip, Paris.

Iffly, R., 1956. Etude de l'écoulement des gaz dans les milieux poreux. Rev. de l'I. F. P. 11, 757–796.

Kalaydjian, F., 1990. Origin and quantification of coupling between relative permeabilities for two-phase flows in porous media. Transport in Porous Media 5, 215–229.

Kaviany, M., 1991. Principles of heat transfer in porous media. Springler Verlag, New York.

Marle, C.M., 1981. Multiphase flow in porous media, éd. Technip, Paris.

Osoba, J.S., Richardson, J.G., Kerver, J.K., Hafford, J.A., Blair, P.M., 1951. Laboratory measurements of relative permeability. Petroleum Transactions AIME 192, 47–56.

Ramakrishnan, T.S., Capiello, A., 1991. A new technique to measure static and dynamic properties of partially saturated porous medium. Chemical Engineering Science 46, 1157–1163.

Richardson, J.G., Kerver, J.K., Hafford, J.A., Osoba, J.S., 1952. Laboratory determination of relative permeability. Petroleum Transactions AIME 195, 187–196.

Rose, W., 1991. Richards' assumptions and Hassler's presumptions. Transport in Porous Media 6, 91–99.

Rose, W., 1988. Measuring transport coefficients necessary for the description of coupled two-phase flow of immiscible fluids in porous media. Transport in Porous Media 3, 163–171.

Rose, W., 1987. Relative permeability. In: Handbook of Petroleum Reservoir Engineering. Society of petroleum engineers, Dallas (Chapter 28).

Whitaker, S., 1986. Flow in porous media, II. The governing equations for immiscible two-phase flow. Transport in Porous Media 1, 105–125.